A 2D numerical model using finite volume method for sediment transport in rivers

E. Peña & J. Fe & J. Puertas
Civil Engineering School, University of A Coruña, A Coruña, Spain

F. Sánchez-Tembleque
Centro de Innovación Tecnolóxica en Edificación e Enxeñería Civil (CITEEC), University of A Coruña, A Coruña, Spain

ABSTRACT: The study of rivers as ecosystems has many fields of research, like the resolution and comprehension of flow and sediment transport *phenomena*. In this communication a 2D numerical model using the Finite Volume Method is presented, throughout a Fortran code including both hydrodynamic and morphological processes. Water depth and the two components of velocity are obtained in the hydrodynamic block. Then, the code enters the morphological block and evolution of bed surface due to erosion and deposition is estimated. A specific tolerance in morphological changes is introduced and, if exceeded, the numerical model turns to the hydrodynamic block to evaluate again the new conditions, and so on. The model is tested and validated with data from PIV and 3D Scanning Technologies in laboratory works at the Civil Engineering School and the CITEEC of the University of A Coruña, Spain.

1 INTRODUCTION

The study of bidimensional *phenomena* including flow and sediment transport has a great importance in many fields of civil engineering. Processes relating to these disciplines have special relevance in all kind of hydraulic works, allowing to analyse the fluvial alterations in the river ecosystem and surroundings.

Fulfilling these studies may be easier with the availability of numerical models to predict the hydrodynamic and morphological variations. The determination of depths, velocities and erosion or sedimentation zones is very important to know the characteristics of the environment and its evolution.

Numerical models capabilities depend on the power of the existing computers. The decrease in the computational time for their application by the international scientific community is a determinant feature. Convergence, stability and an appropriate calibration are necessary to use properly these tools, and validation must be carried out with laboratory experiments and field work. Another important condition when using these models is the adaptation to the selected problem, even more in sediment transport processes, because coherent results may vary according to the mean diameter of the selected sediment (and if this one varies in the domain), a proper formulation of the bedload and suspended load transport, temporal horizon, etc.

This communication presents a bidimensional numerical model uncoupled for flow and sediment transport, with separated explanation and validation results. Both blocks of the developed model are Fortran codes that use the Finite Volume Method (FVM) in discretization and resolution of the representative equations.

2 HYDRODYNAMIC BLOCK

This part of the code develops the FVM to solve the commonly known Shallow Water Equations (SWE). Results in this block are the water depth and the two horizontal components of depth-averaged velocity.

2.1 *Shallow water equations*

Shallow water equations (SWE) are a well-known set of equations that describe the behaviour of flow when the vertical dimension is small compared to the others. They are frequently used in the evaluation of processes related to water flow that take place in channels, rivers and estuaries. SWE can be obtained by integrating the Navier Stokes equations in the vertical direction and making some simplifications like incompressible flow, small slopes and hydrostatic pressure distribution (Chaudhry, 1993). SWE may appear in some slightly different forms, presented here in the next format:

Continuity equation:

$$\frac{\partial h}{\partial t}+\frac{\partial (hu)}{\partial x}+\frac{\partial (hv)}{\partial y}=0 \qquad (1)$$

where: $h(x,y,t)$ = water depth, (u,v) = components of depth-averaged velocity

Dynamic equations:

$$\begin{aligned}\frac{\partial (uh)}{\partial t}+\frac{\partial (u^2 h)}{\partial x}+\frac{\partial (uvh)}{\partial y}&=gh\left(S_{0x}-\frac{\partial h}{\partial x}\right)-ghS_{fx}\\ \frac{\partial (vh)}{\partial t}+\frac{\partial (uvh)}{\partial x}+\frac{\partial (v^2 h)}{\partial y}&=gh\left(S_{0y}-\frac{\partial h}{\partial y}\right)-ghS_{fy}\end{aligned} \qquad (2)$$

where: (S_{0x},S_{0y}) = the geometric slopes; (S_{fx},S_{fy}) = friction slopes, computed with Manning's *formulae*:

$$S_{fx}=\frac{n^2 u\sqrt{u^2+v^2}}{h^{4/3}};\quad S_{fy}=\frac{n^2 v\sqrt{u^2+v^2}}{h^{4/3}} \qquad (3)$$

2.2 *Discretization of domain and equations. Integration.*

Application of FVM in our case comes from a previous triangle mesh discretization. The vertexes of this triangles are the nodes of the final mesh. For a given node N_i we use the barycentres of the triangles that have N_i as a common vertex and the middle point of the triangle side that meets at N_i. The boundary of the cell of the finite volume C_i is then obtained by joining these points together as can be seen in Figure 1. This type of FV appears frequently in scientific literature (Godlewsky and Raviart (1996)).

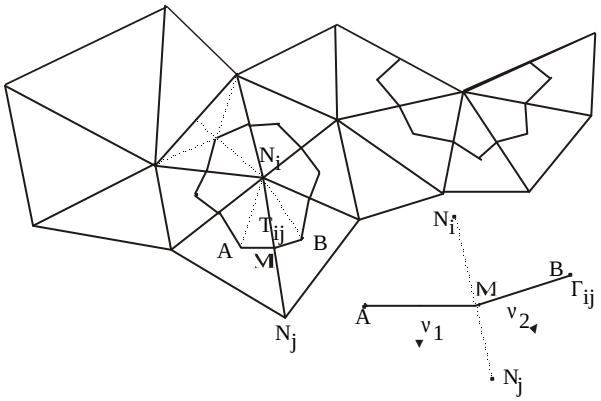

Figure 1. Construction of finite volumes

Working with the SWE in their conservative form and benefit from these equations advantages (Toro, 1997), we carry out a change in notation as follows:

$$\frac{\partial w(x,y,t)}{\partial t}+\frac{\partial F_1(w)}{\partial x}+\frac{\partial F_2(w)}{\partial y}=G(x,y,w) \qquad (4)$$

$$(x,y)\in \Omega\subset R^2;\quad t\in[0,T]$$

where:

$$w=\begin{pmatrix}h\\ hu\\ hv\end{pmatrix};\qquad F_1=\begin{pmatrix}hu\\ hu^2+\frac{1}{2}gh^2\\ huv\end{pmatrix}$$

$$F_2=\begin{pmatrix}hv\\ huv\\ hv^2+\frac{1}{2}gh^2\end{pmatrix};\quad G=\begin{pmatrix}0\\ gh(S_{0x}-S_{fx})\\ gh(S_{0y}-S_{fy})\end{pmatrix}$$

System is written in a more compact form:

$$\frac{\partial w}{\partial t}+\nabla\cdot\mathbf{F}(w)=G(x,y,w) \qquad (5)$$

where:

$$\mathbf{F}(w)=(F_1(w),F_2(w))^T;\quad \nabla\cdot\mathbf{F}=div(\mathbf{F}) \qquad (6)$$

Now we approximate the exact solution of the equations at the time t_n ($t_n = n\Delta t$) by means of the value W_n, constant in every cell and time step. The first term is discretized in advance using the Euler method:

$$\frac{\partial w}{\partial t}\approx\frac{W^{n+1}-W^n}{\Delta t} \qquad (7)$$

Next we integrate the equations over C_i:

$$\begin{aligned}&\iint_{C_i}\frac{W^{n+1}(x,y)-W^n(x,y)}{\Delta t}dA+\iint_{C_i}\nabla\cdot\mathbf{F}(W^n)dA=\\ &\iint_{C_i}G(x,y,W^n)dA\end{aligned} \qquad (8)$$

Using the Theorem of Divergence in the second term we change the integral over C_i into an integral over Γ_i, boundary of C_i.

Taking into account that W_n, W_{n+1} and Δt are constants, they can be carried out of the integral. Flux and source terms required decentre and upwind schemes. To discretize the flux term we follow the Q-scheme of Van Leer, used in Bermúdez *et al* (1998). The discretization of the source term also requires an upwind scheme, as it has been recently analysed in Vázquez (1999) and García Navarro *et al* (2000).

Finally we obtain an explicit in time iterative method allowing us to determinate the variables h, hu and hv in each node N_i at time t_{n+1}, starting from the values of these variables at time t_n in N_i, and the nodes N_j surrounding node N_i.

3 MORPHOLOGICAL BLOCK

As previously stated, this part of the code works uncoupled to the hydrodynamic block. The domain in this part, discretized first in triangles and then in fi-

nite volumes, is exactly the same in order to reduce computational time in solving both processes.
The morphological part of the model uses the previously computed hydrodynamics, so water depth and components of depth-averaged velocity are known. Sediment transport iterations results in evaluation of the bed surface evolution and sediment volumes exchanged between cells. The existing material must be granular and uniform in all the domain, and an unsteady regime is assured as it will be explained afterwards in both blocks interactions.

3.1 *Continuity equation*

The continuity equation for sediment transport by Exner (Exner 1925) allows many kinds of presentation, varying according to the different types of transport. The morphological block calculates the bedload transport with non cohesive sediments, presenting here the mentioned continuity equation from García (García, 2000).

$$(1-p)\frac{\partial z}{\partial t}+\frac{\partial q_{bx}}{\partial x}+\frac{\partial q_{by}}{\partial y}+w_s\left(E_s-\overline{c_b}\right)=0 \qquad (9)$$

where: p = porosity; z = bed surface; (q_{bx},q_{by}) = components of bed load transport; w_s = fall velocity of sediment, E_s = re-suspension factor, c_b = median concentration of sediment in *equilibrium*.
First performances using a centred method led to some instabilities, so an upwind scheme was also used in this part of the model. Surface integral development and divergence theorem application lead to:

$$z^{n+1}=z^n-\frac{\Delta t}{(1-p)}\left[\left(\frac{\sum_{\Gamma_i}\vec{q}_b\cdot d\vec{l}}{A_i}\right)-\left(n_s\cdot\left(E_s-\overline{c_b}\right)\right)\right] \qquad (10)$$

In this case the preceding equation shows an iterative explicit method in time, allowing to obtain the bed surface evolution in each node N_i at any interval, coming from values of the variables in the previous moment, in the node N_i and nodes N_j surrounding it.

3.2 *Equations for bed load transport*

There are many empirical bed load transport equations in the literature. Morphological block of the model was calibrated with different laboratory experiments, using the best relations for the conditions of our studies. In the results included in this paper the analyses have been made with Meyer-Peter&Müller bed load transport formula.

$$\frac{q_{bs}}{\sqrt{(G-1)gd_{50}^3}}=8\left(\theta_*-\theta_{*c}\right)^{1.5} \qquad (11)$$

where: τ_* = non dimensional shear stress, τ_{*c} = non dimensional critical shear stress, d_{50} = mean diameter of sediment, g = gravity, G = specific gravity.

4 COUPLING BLOCKS

The coupling of both parts of the model is as follows. First of all, the hydrodynamic block is run solving the initial hydraulics according to the existing domain and boundary conditions. Reaching a selected convergence, the model enters the morphological block with the computed hydrodynamic data. In this part, the surface evolution (erosion or sedimentation) of the nodes is estimated, until one of them exceeds a significant level (3 d_{50}, depending on d_{50}). When the iteration arrives at this threshold, the model goes back to the hydrodynamic block, estimating new values for hydraulic variables. As convergence is reached again, model goes to morphological block and so on. There is a maximum erosion level introduced by the user, although the model may finish execution, if conditions for erosion or deposition disappear in every point of the mesh at any moment.
The model admits any modification in boundary conditions during the process as a part of an unsteady behaviour, re-estimating hydraulic and morphological variables with these new data. In case of spilling in downstream border with critical depth, the model may modify this boundary condition turning to the introduced level if erosion leads to that.
The real time of the whole process is the correspondent to the morphological block, because the time between iterations in the hydrodynamic one is a time of adaptation, that in reality happens at the same time of morphological processes.

5 RESULTS

Some results of the model are presented here. Although the model is presented in only one Fortran code, hydrodynamic results are presented previously and separately. Then, an example of the full numerical model is included and compared with the experimental results of the same test. The reason is that the hydrodynamic block was first finished and validated before developing the sediment transport subroutines.

5.1 *Hydrodynamic block*

Hydrodynamic part of the model was validated with some particular cases existing in the scientific literature. These examples were not developed with the complete numerical model because of the specific hydraulic problem that they represent, and also because the morphological block is not able to solve some of these particular cases with movable bed.

5.1.1 *Channel with an obstacle at the bottom.*

A 25x1 m laboratory flume is presented with an obstacle of parabolic section at its bottom, unitary discharge of 0.18 m^2/s, downstream depth 0.33 m, Manning's n=0.01 and 505 nodes mesh.

Figure 2 shows the water depth in the axis of symmetry, in order to be able to compare the results of our 2D model with those obtained in a 1D model and the 1D exact solution.

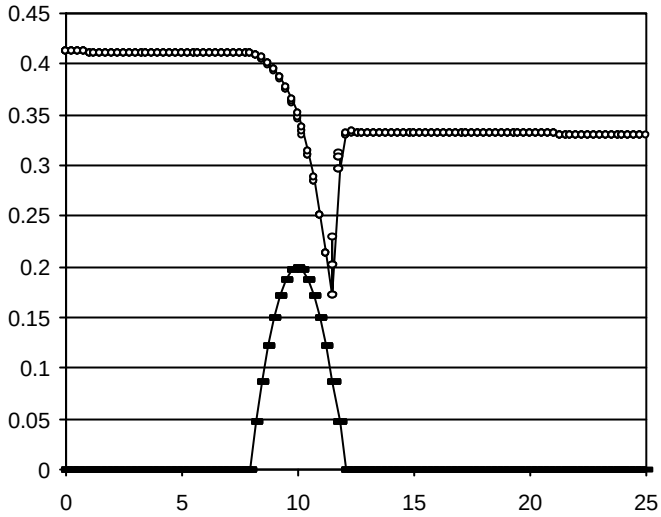

Figure 2. Longitudinal profile (x axis) and depths (y axis) in meters, in a channel with obstacle and with double changing regime.

Due to the presence of the obstacle, it appears a double changing regime, with a clear hydraulic jump in the second one. This result is very similar to the example showed in Vázquez (1999).

5.1.2 *Dam-break problem.*

It is very frequent in scientific literature to use the dam-break problem for the validation of a model. A domain of 5x200 m without friction at the bottom has been considered, ensuring depths of 1 m and 0.1 m as initial conditions in the two separated areas. Again the water depth in the axis of symmetry, at time t = 25 s, is presented. The Δt used (0.2 s) is the maximum one in which there are no oscillations, so is equivalent to Courant´s number for one dimension. Results match very well the exact solution as can be seen in Burguete & García-Navarro (2000).

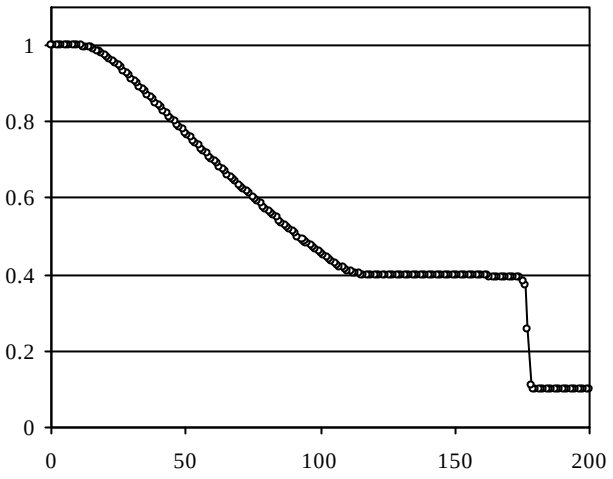

Figure 3. Longitudinal profile (x axis) and depths (y axis) in meters, in a dam-break test in 5x200 m, Δt=0.2 s, t=25 s.

5.1.3 *Settling tanks.*

This example, still without experimental validation, represents a double settling tank with dimensions of 4x3 m, a mesh size of 0.05 m, discharge of 0.1 m^3/s, downstream depth of 0.25 m and Manning's coefficient of 0.014. In Figure 4 we can see the streamlines and eddies properly formed, and fluid separations appearing in different parts of the area in study.

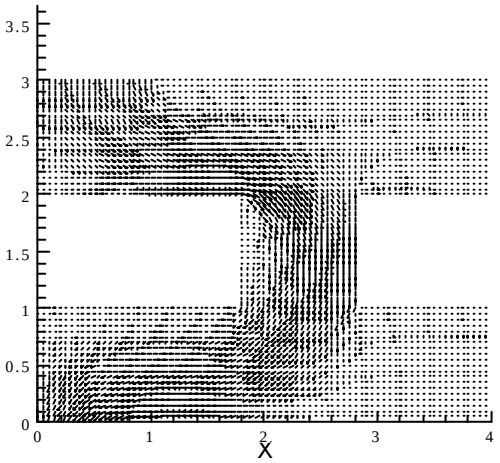

Figure 4. Streamlines in settling tanks of 4x3 m.

5.2 *Morphological block.*

The complete numerical model (including hydrodynamic and morphological blocks) was run and validated with different experimental tests developed in the Civil Engineering School, University of A Coruña, Spain.

The experiment included in this presentation was developed in a 50 x 50 cm, 15 m long current flume. Between two central points of the flume (4.5 and 9.0 meters, from upstream), a volume of sediment of 4 cm height covering the whole cross section was placed, in order to analyse the hydraulic and morphological behaviour until *equilibrium* with a constant discharge. Experimental test last 3 hours until

this condition was reached, with sediment transport towards downstream produced by the bed load. Instrumentation tools included a Particle Image Velocimetry (PIV) to obtain the whole velocity field and depths in the central section, between points 7.6 and 8.3 (in meters, from upstream). Bed surface elevation was obtained from data of PIV and other instrumentation tools.

The following figures present the results of the complete numerical model (hydrodynamic and morphological blocks) and the comparison with the experimental data measured in the mentioned test in the axis of symmetry.

Slope was 0.052%, discharge 21.9 l/s, downstream level 0.12 m, mean diameter of sediment of 1 mm and mesh size of 0.1 m.

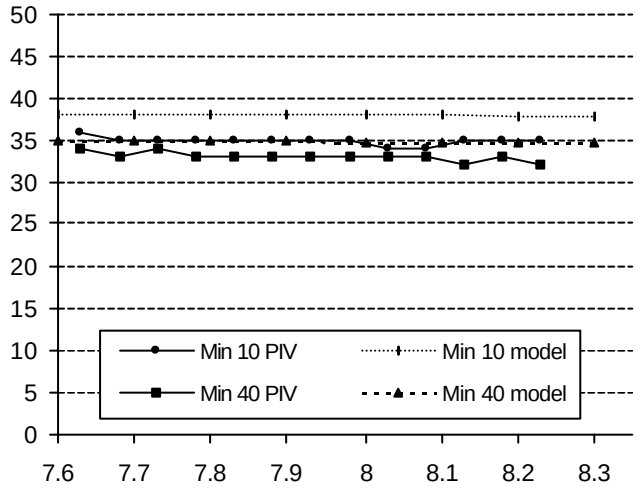

Figure 5. Comparison of experimental and numerical results of bed surface elevation (y axis, in mm) *versus* longitudinal profile (x axis, in m) in two time steps

Figure 5 shows a good agreement of the morphological results and the experimental data for bed surface evolution. It turns out a better accuracy of the model in higher steps of time until equilibrium is reached in both numerical and experimental tests.

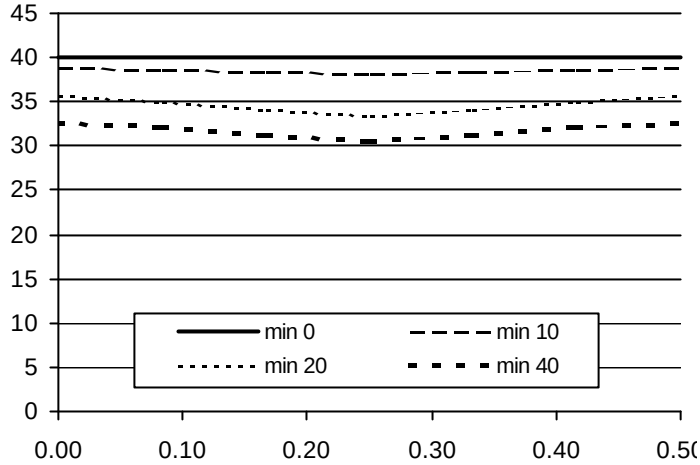

Figure 6. Evolution of bed surface elevation (y axis, in mm) in a cross section located 5.5 meters from upstream the flume (x axis, in m), from beginning to minute 40

Figure 6 also presents a good behaviour of the numerical model representing the bed surface evolution of a certain cross section. Similar results were obtained for the rest of the sediment domain in the central part of the flume.

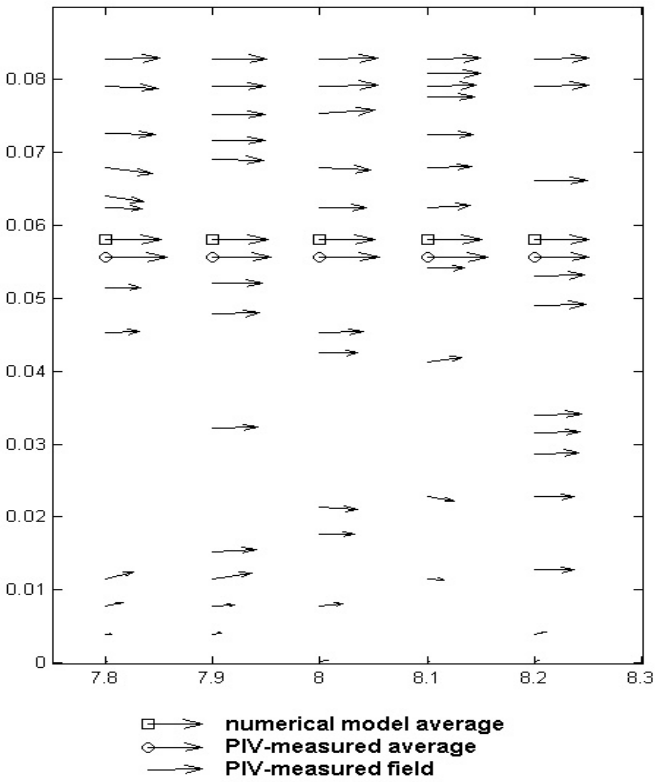

Figure 7. Velocity distribution in longitudinal profile (x axis, in m) *versus* water depth (y axis, in m). Results of depth-averaged velocity of experimental and numerical tests are also plotted.

Last figure points out some differences in velocity distribution results, although similar values of depth-averaged velocity assure the agreement of the hydrodynamic variables of the numerical model with the experimental data.

6 CONCLUSIONS

The present 2D numerical model developing Finite Volume Method and Shallow Water Equations in unsteady flow represent properly the hydrodynamic *phenomena* of many existing problems in scientific literature. Results of the morphological block of the model show the agreement of the bed surface evolution compared with data from laboratory experiments, applying laser instrumentation as Particle Image Velocimetry. Upwind schemes are used to assure convergence and stability in both parts of the model, and Meyer-Peter&Müller bed load transport formula is found accurate to represent sediment transport evolution.

REFERENCES

Burguete, J. & García-Navarro, P. 2000. An upwind conservative treatment of source terms in shallow water equations. *European Congress on Computational Methods in Applied Sciences and Engineering, Eccomas 2000, Barcelona (Spain)*

Bermúdez, A. & Dervieux, A. & Desideri, J.A. & Vázquez-Cendón, M.E. 1998. Upwind schemes for the two-dimensional shallow water equations with variable depth using unstructured meshes. *In Elsevier Science Publishers, Computer Methods in Applied Mechanics and Engineering 155:49-72. Amsterdam (The Netherlands)*

Chaudhry, M. 1993. Open channel flow. *Prentice-Hall, Inc., New Jersey (USA)*

Einstein, H.A. 1950. The bedload function for bedload transportation in open channel flows. *Technical Bulletin No. 1026, USDA, Soil Conservation Service. USA*

Exner, F.M.1925. Über die wechselwirkung zwischen wasser und geschiebe in flüssen. *Sitzenberichte der Academie der Wissenschaften, Sec. IIA:134-199. Wien (Austria)*

García, M. & Parker G. 1991. Entrainment of bed sediment into suspension. *In American Society of Civil Engineer, Journal of Hydraulic Engineering* 117:414-435

García, M. 2000. Sedimentation and erosion hydraulics. *Hydraulic Design Handbook, to be published by Mc Graw Hill.*

García-Navarro, P. & Vázquez-Cendón, M. E. 2000 On numerical treatment of the source terms in the shallow water equations. *Computers & Fluids 29 (2000) 951-979.*

Godlewsky, E. & Raviart, P. 1996. Numerical approximation of Hyperbolic Systems of Conservation Laws. *Springer-Verlag, Berlin*

Meyer-Peter, E. & Müller, R. 1948. Formulas for bedload transport. *Proceedings of the 2nd Congress of the International Association for Hydraulic Research, Stockholm,* 39-64

Toro, E.F. 1997. Riemann Solvers and Numerical Methods for fluid Dynamics. *A practical introduction. Springer-Verlag, Berlin*

Van Rijn, L.C. 1993. Principles of sediment transport in rivers, estuaries and coastal seas. *Aqua Publications, Amsterdam (The Netherlands)*

Vázquez-Cendón, M.E. 1994. Estudio de esquemas descentrados para su aplicación a las leyes de conservación hiperbólicas con términos fuente. *Ph.D. Dissertation, University of Santiago de Compostela, Spain*

Vázquez-Cendón, M.E. 1999. Improved treatment of source terms in upwind schemes for the shallow water equations ins channels with irregular geometry. *Journal of Computational Physics* 148:497-526

Versteeg, H.K. & Malalasekera, W. 1995. An introduction to computational fluid dynamics. *The finite volume method. Addison Wesley Longman Ltd. Essex (England)*